

377-27  
52256  
68

# FREE-SURFACE AND CONTACT LINE MOTION OF LIQUID IN MICROGRAVITY

Leonard W. Schwartz

Departments of Mechanical Engineering and Mathematical Sciences

The University of Delaware

Newark, DE 19716

## ABSTRACT

This project involves fundamental studies of the role of nonlinearity in determining the motion of liquid masses under the principal influences of surface tension, viscosity and inertia. Issues to be explored are relevant to aspects of terrestrial processes, as well as being immediately applicable to fluid management in a low-gravity environment. Specific issues include (i) the mechanics of liquid masses in large-amplitude motions, (ii) the influence of bounding surfaces on the motion and (iii) the ability of such surfaces to control liquid motion by wetting forces, especially when they are augmented by various surface treatments. Mathematical techniques include asymptotic analysis of the governing equations, for problem simplification, and numerical simulation, using both boundary-element and finite-difference methods. The flow problem is divided into an 'outer' or inviscid potential-flow region and one or more inner, or viscous dominated, regions. Relevant to one inner region, the vicinity of the contact line, we discuss time-dependent simulation of slow droplet motion, on a surface of variable wettability, using the lubrication approximation. The simulation uses a disjoining pressure model and reproduces realistic wetting-dewetting behavior.

## INTRODUCTION

From an engineering viewpoint, it is often necessary to maintain the location of a quantity of liquid in an enclosed vessel. This task is made simple in terrestrial gravity where the liquid in a partially-filled container can naturally be assumed to locate itself near the 'bottom' of the vessel. In the absence of gravity, however, it is possible for a liquid mass to become disconnected and become intermixed with its own vapor in an a priori unpredictable manner. Similarly, when the stabilizing gravitational potential is not present, the center of mass of a liquid region may move a large distance when disturbed by relatively small applied forces, with influence on the overall dynamics of a space vehicle.

Liquid motion in microgravity allows a more complete examination of surface tension and wetting forces. In normal gravity, capillary forces are restricted to short length scales and their influence, while important, is often obscured by the concurrent high level of viscous damping. When terrestrial gravity is removed, the spatial extent of capillary-dominated regions is greatly magnified and more detailed measurement is possible.

A strategy for control of liquid motion involves the location and surface treatment of container walls. The motion of a liquid front on a solid surface is governed in part by the energetics of the three interfaces that meet at the so-called contact line. A local force balance specifies the static contact angle between the phases there. Terrestrial experiments have indicated surprisingly high rates of damping of liquid motions which has been attributed to energy dissipation at moving contact lines [1]. For a surface whose energies vary with position, e.g. if the surface is 'contaminated,' it is possible for the contact line to be trapped in various local energy minima leading to a significant difference, or hysteresis, between advancing and receding contact angles [2]. Forced motion of the contact line on these surfaces will require a succession of small energy barriers to be overcome and may provide sufficient dissipation to prevent large motions. Quasi-static analyses by Schwartz & Garoff [3,4] considered various patterns of surface wettability. Some of their predictions were confirmed experimentally. Those results are only appropriate to very slow imposed motions. One goal of the present project is the extension to finite speed, where viscous forces must also be considered. Small scale roughness is believed to play a role similar to surface contamination [5].

## THE LARGE-SCALE INVISCID PROBLEM

Large-scale oscillations of liquid masses involve, principally, interchange between the kinetic energy of motion and potential energy stored as elongation of the bounding surface. Solutions for wave motions of infinitesimal amplitude are well known. For example, the small-amplitude oscillation of a liquid droplet was predicted by Rayleigh in 1877 [6]. Large amplitude motions, on the other hand, are highly nonlinear and will, in general, require numerical solution. Sloshing motions of low viscosity liquids in tanks of moderate or large size may, away from the walls and contact lines, be considered to be irrotational potential flows. The potential  $\phi$  is found as the solution of Laplace's equation

$$\nabla^2 \phi = 0, \quad (2.1)$$

subject to the kinematic boundary condition

$$DF/Dt = 0 \quad (2.2)$$

on the free interface  $F(x, y, z, t) = 0$ . Here  $D/Dt$  is the substantial derivative. The solution must also satisfy the condition of no normal relative velocity at stationary or moving impermeable boundaries. Additionally, on the free surface, whose shape evolution needs to be found as part of the solution, we have the dynamic condition

$$\phi_t + (1/2)(\phi_x^2 + \phi_y^2 + \phi_z^2) + \frac{p^{(s)}}{\rho} + \sigma \left( \frac{1}{R_1} + \frac{1}{R_2} \right) = C(t). \quad (2.3)$$

Here  $\rho$  is the constant liquid density,  $\sigma$  is surface tension, and  $C(t)$  is a function of time only.  $R_1$  and  $R_2$  are principal radii of curvature. The applied surface pressure  $p^{(s)}$  is ordinarily taken equal to zero without loss of generality; here, however, it may be used to represent the far-field influence of the 'inner' moving contact-line problem. Time-dependent solutions of (2.1) - (2.3) can be achieved using boundary-integral methods for two-dimensional or axisymmetric problems. These techniques find generalization in the so-called panel methods for three-dimensional problems. An example of a boundary-integral solution to a two-dimensional problem is shown in Fig. 1 where a limiting wave form traps a vapor bubble [7].

## DROPLET MOTION ON SUBSTRATES OF MIXED WETTABILITY

We treat the low-Reynolds-number motion of a thin Newtonian liquid layer onto a previously-dry surface. The mathematical model employs the long-wave or "lubrication" approximation. To leading order in the free-surface inclination, only a one-dimensional, unidirectional flow problem needs to be solved. Performing this integration across the thin dimension first results in a reduction of the dimensionality of the problem. Consistent with the lubrication hypothesis, many physical effects of interest can be modeled much more simply. Asymptotic derivations of the lubrication model, for two-dimensional problems with a free surface, are given by Benney [8] and Atherton & Homsy [9].

Within this approximation, integral mass conservation and the creeping-motion force balance are combined to yield

$$h_t = -\nabla \cdot \mathbf{Q} = \frac{1}{3\mu} \nabla \cdot (h^3 \nabla p) \quad (3.1)$$

where

$$p = -\sigma \nabla^2 h - \Pi = -\sigma \nabla^2 h - B \left( \frac{1}{4h^4} - \frac{1}{3h^* h^3} \right) \quad (3.2)$$

Here  $h$  is the coating thickness,  $p$  is pressure and  $\mu$  is viscosity. The  $\nabla$  - operator is two-dimensional, and is written using the substrate coordinates, and  $t$  is time. The first term in (3.2) incorporates the thin-layer approximation to the surface curvature while the second is a two-term model of disjoining pressure that allows contact-line motion, as described below.  $B$  and  $h^*$  are positive constants. The form of the disjoining term depends on the material system. Teletzke et al give various choices including the one used here [10]. Several flow simulations, using a form of disjoining pressure, have appeared [10,11].

When a liquid advances onto a previously-dry substrate, the usual mathematical description of the motion fails in the immediate vicinity of the three-phase line, i.e. the line where the liquid, solid, and

the vapor meet. The standard boundary condition, when a viscous liquid is in contact with a solid, is no relative motion between the liquid and the solid, the so-called 'no-slip' condition. It has been shown that solutions incorporating the no-slip condition lead to paradoxical results; the work required to move a liquid onto a dry surface is infinite [12,13]. Clearly the no-slip condition must be abandoned very near the moving contact point or line. Several slip models, involving a free parameter, have been proposed [14,15,16]. Other possibilities are a uniform precursor layer [17], a grid-slip model that allows motion onto dry regions, with the rate of advance dependent on the numerical mesh spacing [18], and shear-thinning rheology near the contact line [19]. Figures (2a) and (2b) show calculations for liquids advancing onto nominally-dry substrates. Figure (2a) shows the development of fingers or drip marks for gravity-driven flow on a vertical substrate [18]. Figure (2b), using a uniform precursor layer, simulates finger development on a spherical body.

The inclusion of the the disjoining terms in (3.2) is another technique that will allow contact-line motion using a thin wetting layer. Consider the spreading of an initially axisymmetric droplet onto a nominally-dry substrate. The evolution equation is nondimensionalized by measuring  $h$  in units of  $h_0$ , a typical film thickness. The substrate coordinates  $(x, y)$  are measured in units of  $L$  and the unit of time is  $T^* = 3\mu L^4/(\sigma h_0^3)$ . In dimensionless form, the evolution equation is

$$h_t = -\nabla \cdot (h^3 \nabla \nabla^2 h) + C \nabla \cdot \left[ \left( 1 - \frac{h}{h^*} \right) \frac{\nabla h}{h^2} \right] \quad (3.3)$$

where

$$C = \frac{BL^2}{\sigma h_0^5} \quad (3.4)$$

The now-dimensionless parameter  $h^* \ll 1$  and, for droplet spreading, when combined with the value of  $C$ , prescribes the value of the equilibrium contact angle on a given substrate material. The energy per unit area of the substrate is composed of two parts. Within the lubrication approximation, the surface tension energy density is

$$e^{(s)} = \frac{1}{2} \sigma \nabla h \cdot \nabla h \quad (3.5a)$$

and the disjoining energy density is

$$e^{(d)} = - \int_{\frac{3}{4}h^*}^h \Pi(h') dh' = \frac{B}{6h^{*3}} \left[ \frac{16}{27} - \frac{h^{*2}}{h^2} \left( 1 - \frac{h^*}{2h} \right) \right] \quad (3.5b)$$

both in dimensional units.  $e^{(d)}$  has a minimum at  $h = (3/4)h^*$  and (3.5b) is normalized so that  $e^{(d)}$  is zero there. It is possible to identify the value of  $B/h^{*3}$  with the equilibrium contact angle. For a static situation,  $e_{SV}^{(d)} = e^{(d)}(3h^*/4) = 0$  and  $e_{SL}^{(d)} = e^{(d)}(h \rightarrow \infty)$  when  $h^*$  is very small. A local force balance at the contact point gives

$$\sigma \cos \theta_c = \gamma_{SV} - \gamma_{SL} = \sigma - \frac{8}{81} \left( \frac{B}{h^{*3}} \right) \quad (3.6)$$

which, consistent with the small-slope approximation, yields

$$\theta_c \approx \frac{4}{9} \left( \frac{B}{\sigma h^{*3}} \right)^{1/2} \quad (3.7)$$

Here the subscripts S, L, and V have their usual meaning of solid, liquid, and vapor respectively. Since  $\theta_c$  is the material property to be reproduced, constancy of the quantity  $C/h^{*3}$  is to be maintained as  $h^*$  becomes small. Provided  $h^*$  is taken sufficiently small, simulation results become independent of its actual value. Numerical tests reveal that a droplet will stabilize with a maximum inclination approximately given by (3.7), smaller values of  $h^*$  producing closer agreement. In this sense the actual value of  $h^*$  is not needed; the only material property required is the apparent static contact angle.

Few surfaces are ever ideally clean. Moreover, one may wish to purposely place patterns of contamination on a substrate in order to arrest liquid motion. Equation (3.3) is capable of simulating such a situation by

prescribing different values of  $C$  in particular substrate locations. Figure 3 shows the result of a time-dependent simulation where a drop of non-equilibrium shape is placed approximately at the center of a "cross" of poor-wetting material. The contact angle, using (3.7) is twice as large on the cross, compared to the surrounding field. Reflection symmetry conditions are used at the boundaries of the computational domain. Figure 4 contains contour plots of the same simulation with the wettability boundaries superimposed. Rather realistic features are exhibited by the simulation; apparent advancing and receding contact angles are speed-dependent and the motion proceeds by alternating slow and rapid events. This is readily seen in Figure 5 where the variation of the integrated energy components, using (3.5), is shown. This is similar to the result of the quasi-static analyses of Schwartz & Garoff [3,4] who termed the process "sticking, stretching, and jumping" in their model of contact-angle hysteresis. The simulation ends with the droplet finding a stable energy minimum by merging with its neighbors in one corner. The rate of decrease of the total energy in Figure 5 can be shown to be equal to the rate of viscous dissipation. Notice that when the motion has ceased, the energy is approximately equally-partitioned between its two components.

These computations use an alternating-direction-implicit (ADI) algorithm based on the scheme of Peaceman & Rachford [20], generalized to the present higher-order diffusive system. Nonlinearity is treated simply by evaluating prefactors at the old time level. The algorithm is quite stable and time stepping is adaptive, with larger steps being used when the surface shape is changing slowly. Steps can be as large as a factor of  $10^7$  bigger than the limiting step size for an explicit method. Basic features of the simulation have been verified to be invariant under temporal and spatial refinement and the choice of values for  $h^*$ . Additional tests of convergence are currently in progress. The run shown here, using a  $100 \times 100$  finite-difference grid, took about 30 minutes on a Pentium 100 PC configured as a UNIX workstation.

We intend to consider other disjoining pressure models to assess the sensitivity of flow behavior to this choice. Physical experiments on surfaces of controlled wettability can be compared with numerical predictions. For relatively large drops, in the laboratory, gravity effects will need to be considered. These can be inserted in the model without difficulty.

## REFERENCES

1. Keulegan, G. H. (1959), *J. Fluid Mech* 6, 33-50.
2. Johnson, R. E. & Dettre, R. H. (1969), *Surf. Colloid Sci.* 2, 85.
3. Schwartz, L. W. & S. Garoff (1985a), *J. Colloid Interf. Sci.* 106, 422 - 437.
4. Schwartz, L. W. & S. Garoff (1985b), *Langmuir* 1, 219 - 230.
5. Dussan V., E. B., *Ann. Rev. Fluid Mech.* 11, 371-400.
6. Rayleigh, Lord, (1877) "Theory of Sound," Dover Books, New York, 1945.
7. Schwartz, L. W. & Vanden-Broeck, J.-M. (1979) *J. Fluid Mech.* 95, 119-139.
8. Benney, D. J. (1966) , *J. Math. & Phys.* 45, 150-155.
9. Atherton, R. W. & Homsy, G. M. (1976), *Chem. Eng. Comm.* 2, 57-77.
10. Teletzke, G., Davis, H. T. & Scriven, L. E. (1987) *Chem. Eng. Comm.* 55, 41-81.
11. Williams, M. B. & Davis, S. H. (1982), *J. Colloid Interf. Sci.* 90, 220-228.
12. Moffatt, H. K. (1964), *J. Fluid Mechanics* 18, 1-17.
13. Huh, C. & Scriven, L. E. (1971), *J. Coll. Interf. Sci.* 35, 85-101, 1971.
14. Greenspan, H. P. & McCay, B. M. (1981), *Studies in Applied Mathematics* 64, 95-112.
15. Hocking, L. M. (1983), *Quart. J. of Mechanics & Appl. Maths* 36, 55-69, 1983.
16. Durbin, P. A. (1988), *J. Fluid Mech.* 197, 157-169.
17. Tuck, E. O. & Schwartz, L. W. (1990), *S.I.A.M. Review* 32, 453-469.
18. Schwartz, L. W. (1989), *Phys. Fluids A1*, 443-445.
19. Weidner, D. E. & Schwartz, L. W. (1994) *Physics of Fluids* 6, 3535-3538.
20. Peaceman, D. W. & Rachford, H. H. (1955), *SIAM Journal* 3, 28-41.

## FIGURES

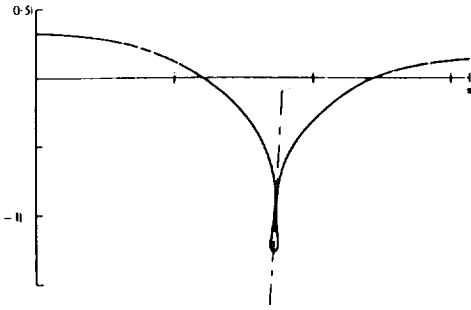


Fig. 1: A capillary-dominant progressive free-surface wave calculated by a boundary-integral method. A bubble is trapped [7].

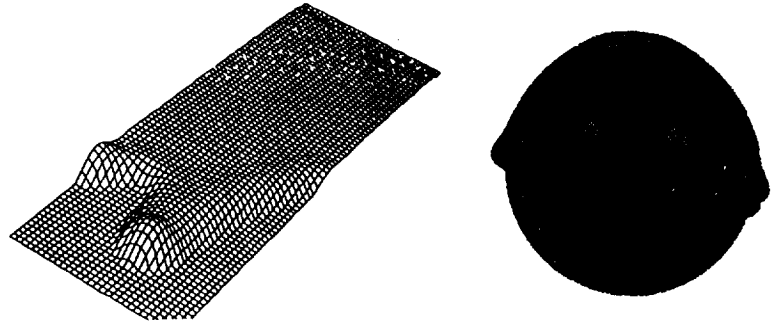


Fig 2: Flow simulations using two different wetting models. (a) A liquid mound on a vertical wall shows characteristic fingering patterns [18]. (b) Drainage on a sphere, using a uniform precursor layer.

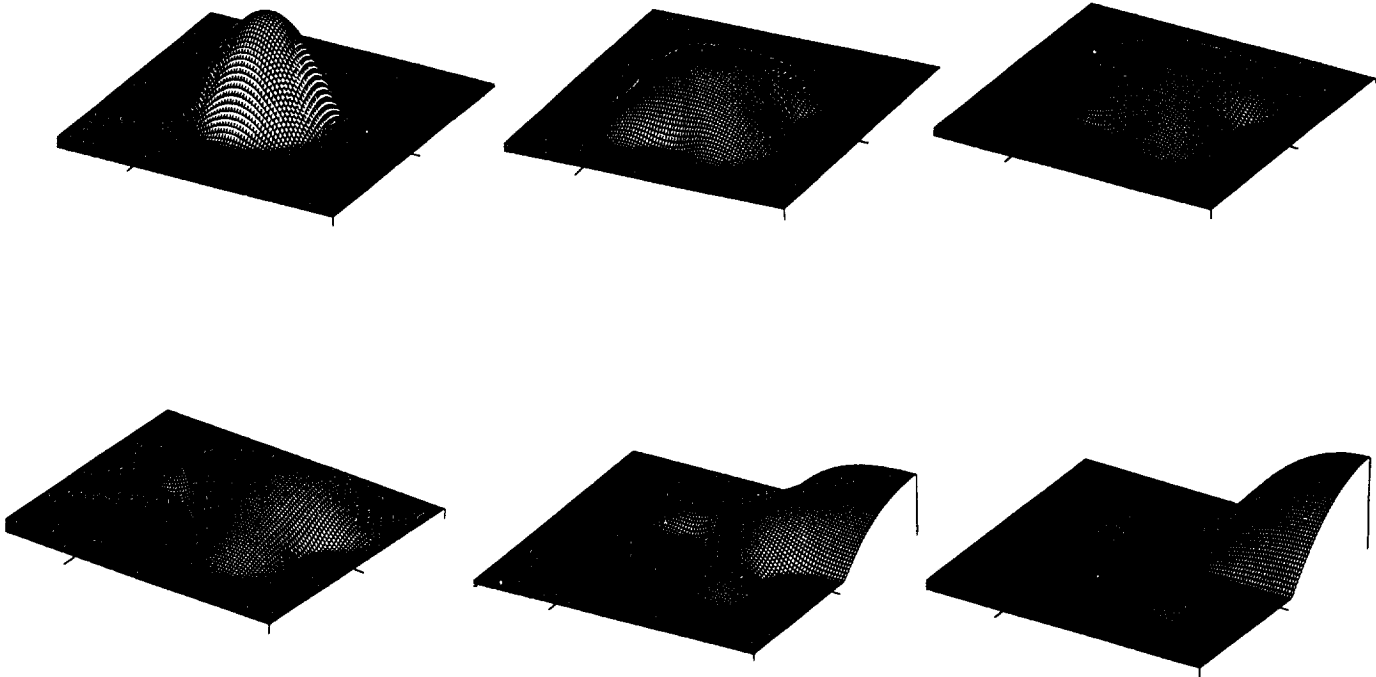


Fig 3: Simulation of droplet motion on a mixed-wettable surface. Parameter values are  $C_1 = 0.0002$ ,  $C_2 = (1/4) C_1$ ,  $h^* = 0.02$ . The grid size is  $0.01 L$  where  $L$  is the width of the window. Times are  $t/T^* = .001, .5, 4., 5. 6., 7$ . The initial profile was  $h = (3/4)[ h^* + \exp(-64 r^2) ]$ .

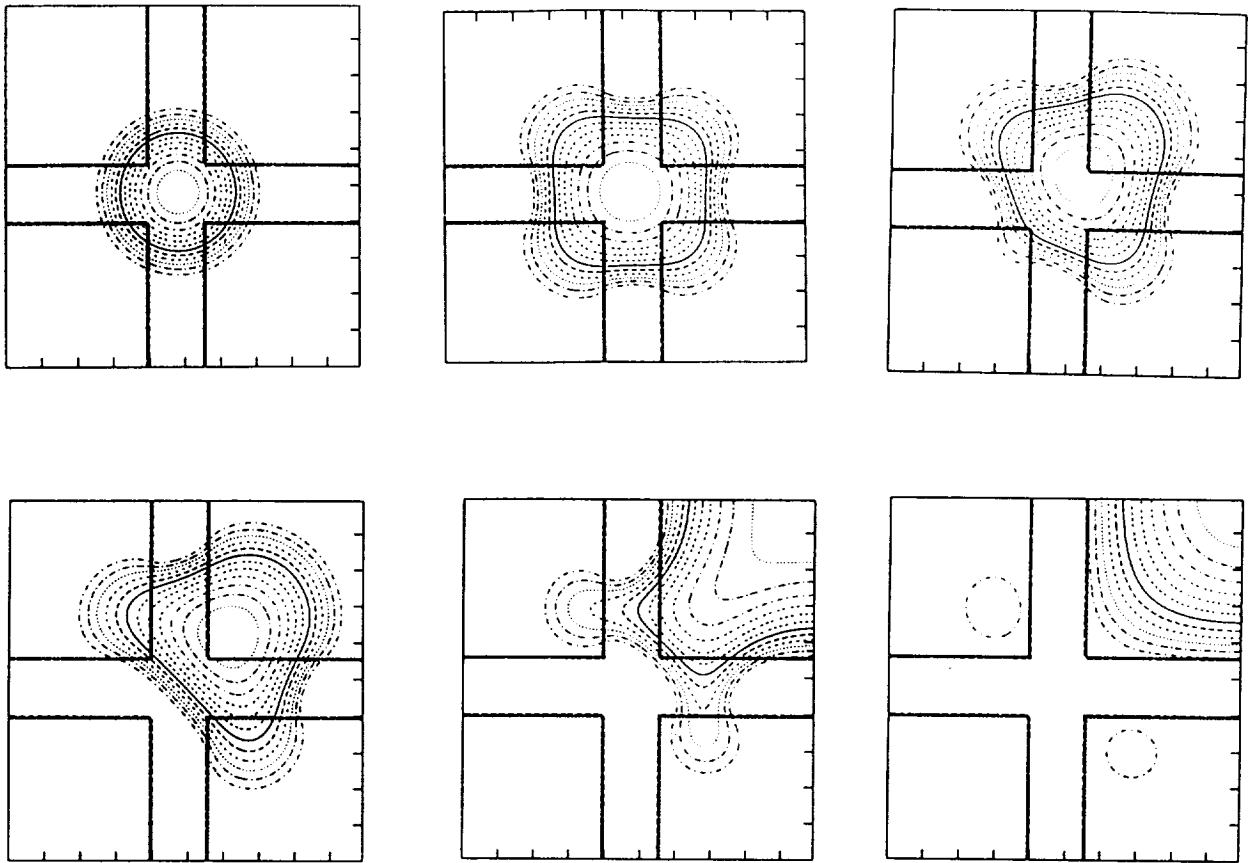


Fig 4: Contour plots for the profiles in Fig. 3 . The wettability boundaries are also shown.

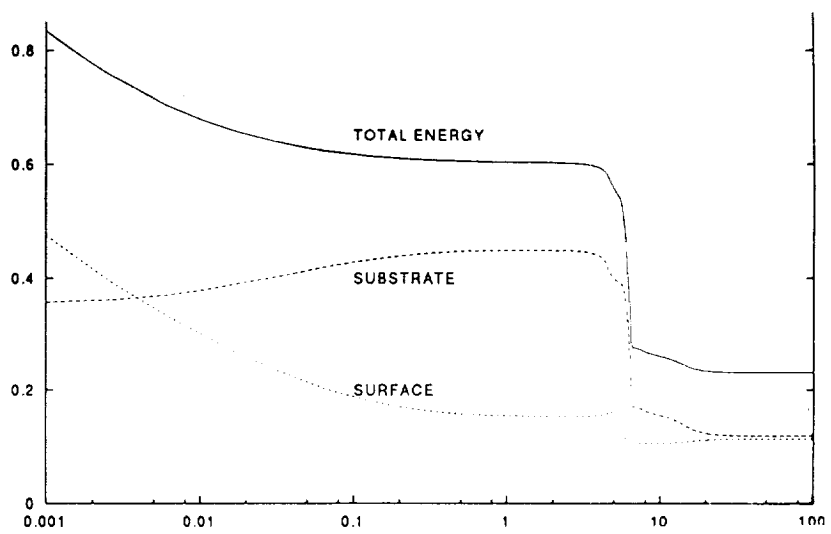


Fig. 5: Variation in integrated energies with  $t/T^*$ . The motion proceeds by alternating fast and slow events. Energies are measured in units of  $\sigma h_0^2$ .